

## MICROINDENTATION TESTS AND MICROABRASIVE BEHAVIOR OF TUNGSTEN COMPOSITES<sup>1</sup>

Gabriel Haddad Souza Gava<sup>2</sup>

Roberto Martins de Souza<sup>3</sup>

Marcelo Camargo Severo de Macêdo<sup>4</sup>

Cherlio Scandian<sup>5</sup>

### Abstract

This work intends to evaluate a possible relationship between the mechanical properties calculated from instrumented microindentation data and the microabrasive wear behavior of infiltrated tungsten (W) composites used in impregnated diamond bits for rock drilling. Specimens of brass-infiltrated W composites were sintered with combinations of different W particle sizes. After metallographic preparation, specimens were analyzed in an instrumented microindenter with a Vickers indenter. All phases were indented with a load of 30 mN. The indentation curves allowed the calculation of microhardness and Young's modulus for each phase. These results were compared with abrasive wear coefficients obtained in a previous work. It was observed a decrease in microhardness as the tungsten grain size increases. For the SiC abrasive slurry, a decrease in microabrasive wear coefficient followed the decrease in tungsten microhardness. The opposite was observed with the SiO<sub>2</sub> slurry, whereas, for the Fe<sub>2</sub>O<sub>3</sub> slurry, no clear correlation was obtained. Also it is important to say that the effect of infiltrated brass (binder phase) hardness became more significant in the tests with the SiO<sub>2</sub> and Fe<sub>2</sub>O<sub>3</sub> slurries. Depending on the abrasive type, the observed mechanisms were grooving, particles rolling (multiple indentations), besides the occurrence of both simultaneously, although, dissociated.

**Keywords:** Microhardness; Microabrasion; Brass-infiltrated W composites.

### ENSAIO DE MICROPENETRAÇÃO E COMPORTAMENTO EM MICROABRASÃO DE COMPÓSITOS A BASE DE TUNGSTÊNIO

#### Resumo

Este trabalho tem o objetivo de avaliar uma possível relação entre as propriedades mecânicas calculadas a partir dos dados de micropenetração instrumentada e o comportamento do desgaste microabrasivo dos compósitos infiltrados à base de tungstênio (W) usados em coroas diamantadas utilizadas em sondagem mineral. As amostras dos compósitos de tungstênio foram sinterizadas com combinações de diferentes tamanhos de partículas W. Após a preparação metalográfica, as amostras foram analisadas em um micropenetrador instrumentado com um penetrador do tipo Vickers. As fases foram penetradas com uma carga de 30 mN. As curvas geradas a cada penetração permitiram calcular a microdureza e o módulo de elasticidade para cada fase. Estes resultados foram comparados com os coeficientes de desgaste abrasivo obtidos em um trabalho anterior. Foi observada uma diminuição na microdureza conforme o tamanho dos grãos de tungstênio aumenta. Para a lama abrasiva contendo SiC, uma diminuição no coeficiente de desgaste microabrasivo se seguiu à diminuição na microdureza do tungstênio. O oposto foi observado com a lama de SiO<sub>2</sub>, enquanto, para a lama de Fe<sub>2</sub>O<sub>3</sub>, nenhuma correlação clara foi obtida. Também é importante dizer que o efeito da dureza do latão infiltrado (fase aglutinante) tornou-se mais significativa nos ensaios com as pastas de SiO<sub>2</sub> e de Fe<sub>2</sub>O<sub>3</sub>. Dependendo do tipo do abrasivo, os mecanismos observados foram riscamento, rolamento de partículas (múltiplas indentações), além da ocorrência de ambos simultaneamente, embora dissociados.

**Palavras-chave:** Microdureza; Microabrasão; Compósitos; Tungstênio.

<sup>1</sup> Technical contribution to the First International Brazilian Conference on Tribology – TribobR-2010, November, 24<sup>th</sup>-26<sup>th</sup>, 2010, Rio de Janeiro, RJ, Brazil.

<sup>2</sup> Student - PPGEM, UFES – ES, ghsg@bol.com.br

<sup>3</sup> Dr. PPGEM/USP – SP, roberto.souza@poli.usp.br

<sup>4</sup> Dr. PPGEM/UFES – ES, mcamargo@npd.ufes.br

<sup>5</sup> Dr. PPGEM/UFES – ES, cherlio@hotmail.com



## 1 INTRODUCTION

On rock drilling core sample collection, it's important that the impregnated diamond bit is wisely worn, allowing the cutting process to be effective. To accomplish this step, are employed, usually, diamond bits, or, also called, drill bits. These bits are manufactured through the process of sintering by infiltration, which basically consists of a metallic matrix with dispersed small diamonds at random – that is, a composite. The metallic matrixes, formed by a compact amalgam of tungsten powders joint by an infiltrant alloy (in this case, the brass), aim to give support to the diamonds while being worn, in order to expose them during the use of the tool. However, this wear may not be very high because the diamonds would be torn easily.<sup>(1,2)</sup>

It is known that hardness has an important role in abrasive wear behavior. Depending on the wear mechanism, the higher the hardness, the higher is the wear resistance.

Previously, Lozzer<sup>(3)</sup> had tested four specimens of tungsten-based matrixes in a free ball microabrasion equipment (Calowear) with three different types of abrasive slurry ( $\text{SiC}$ ,  $\text{SiO}_2$  and  $\text{Fe}_2\text{O}_3$ ) and compared the dimensional wear coefficient with the macrohardness.

Nevertheless, the results show that there was not always a relationship between hardness and abrasive wear.

In this work, another approach has been studied because of the fact that the specimens present multi-phase microstructures and thus, show, probably, micrometric scale wear mechanisms, with distinct characteristics. Using the instrumented indentation testing technique, also known as depth-sensing indentation, it is possible to obtain the hardness for each presented phase and compare the results with the microabrasive coefficient, the mean tungsten grain size and the wear mechanisms involved, obtained by scanning electronic microscopy.

In contrast to traditional hardness testers, instrumented indentation systems allow the applications of a specified force or a displacement history, such that force ( $P$ ) and the displacement ( $h$ ) are controlled and/or measured simultaneously and continuously over a complete loading-unloading cycle,<sup>(4)</sup> as illustrated in Figure 1.

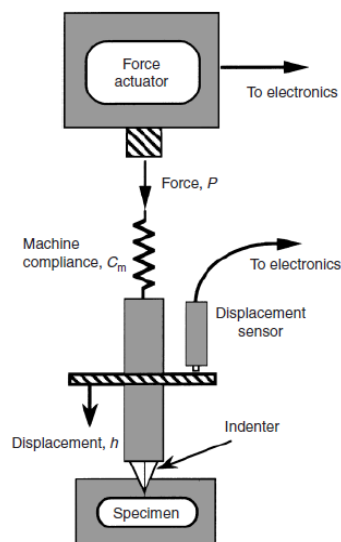


**Figure 1** – Schematic representation of the basic components of an instrumented indentation testing system.<sup>(5)</sup>

An important advantage of instrumented indentation testing results from the fact that load-displacement data can be used to determine mechanical properties, without having to image the hardness impressions. This could allow property measurements at very small scales.<sup>(5)</sup>

During the instrumented indentation test, an indenter is pressed against the specimen surface, and then an elastic-plastic deformation occurs, which results in an impression that depends on the indenter geometry. After a complete cycle, only the elastic portion is recovered. Micro or nano impression printings are very difficult and, thus, the technique has been widely adopted and used in the characterization of small-scale mechanical behavior.<sup>(6)</sup>

A simple methodology has been proposed by Oliver and Pharr<sup>(7)</sup> for the hardness measurement ( $H$ ). This iterative method allows the determination of the area function, which relates the cross sectional area to the distance from its tip, and the machine compliance. The method is based on the measurement of contact stiffness and does not require obtaining a picture of the indentation.

Later, Meza et al.<sup>(8)</sup> improved the above-mentioned technique in relation to tip roundness, initial contact depth, thermal drift, contact stiffness and unloading curve.

## 2 MATERIALS AND METHODS

The specimens are identified according the tungsten mean grain size (4, 6, mixed 6 + 16 and 16  $\mu\text{m}$ ) and have been sintered at 1050 °C with the infiltrating alloy Cu-43Zn-1Sn (% in weight), without diamonds.

The samples were grounded following the sequence of: 220, 320, 400, 600 and 1200. The polishing was performed with a Monocrystalline Diamond Suspension of 1  $\mu\text{m}$  (Buehler).

In this study, tests were carried out in an instrumented Fischerscope microindenter and using a Vickers indenter, as shown in Figure 2.

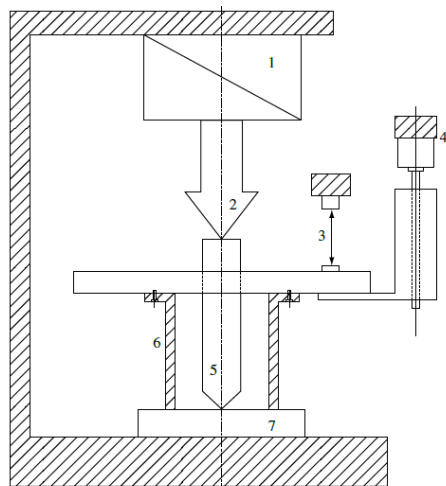


**Figure 2** – (a) schematic representation of head system measurement of a Fischerscope H100V machine: 1) electro-magnetically load system; 2) force; 3) displacement sensor; 4) motor; 5) indenter; 6) reference ring; and 7) specimen;<sup>(8)</sup> (b) Fischerscope H100V machine.

The load test is of 30 mN (3 gf) and fifteen hardness measurements were made for both phases.

As for the instrumentation, the equipment uses the "Microindentation Program H100-HCU" version 2.1E of March 20, 1998.

### 3 RESULTS AND DISCUSSIONS

In Figure 3, the general microstructure of the sintered material is emphasized, where light particles are tungsten powders, whose original average size is of 4  $\mu\text{m}$ , and the dark portion is the infiltrant alloy, Cu-43Zn-1Sn (% in weight). It may be noted that there was some coarsening of tungsten particles during the liquid phase sintering.

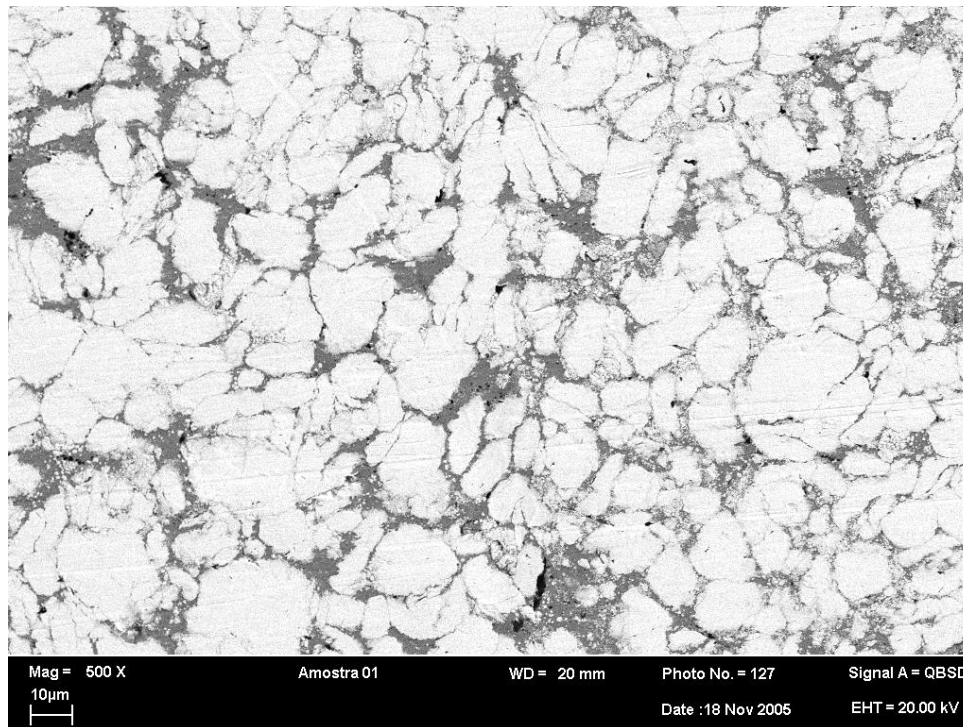


**Figure 3** – Electronic scanning micrography showing the general appearance of the sample.<sup>(3)</sup>

From microabrasion tests on a Calowear-type equipment, [3] obtained results of dimensional wear coefficient  $k$ , for each abrasive slurry, as shown in Table 2:

**Table 2** – dimensional wear coefficients obtained from microabrasion tests with three different types of abrasive slurry<sup>(3)</sup>

Sample ( $\mu\text{m}$ )	Dimensional wear coefficient $k$ , [ $\text{m}^2/\text{N}$ ], for each abrasive slurry		
	SiC	SiO <sub>2</sub>	Fe <sub>2</sub> O <sub>3</sub>
4	4.82 E-12	5.61 E-13	7.45 E-14
6	4.36 E-12	6.36 E-13	6.42 E-14
6+16	4.13 E-12	7.91 E-13	5.82 E-14
16	3.99 E-12	7.10 E-13	6.96 E-14

Wear results present several orders of difference according to the type of abrasive particle, as could be seen in Table 2 and Table 3. The wear severity is higher for SiC and the lower wear rate is obtained for Fe<sub>2</sub>O<sub>3</sub> particles.

**Table 3** – Relationship between average wear coefficients, average hardness of the abrasives,  $H_{\text{AbrasiveSlurry}}/H_{\text{Phase}}$  relationship, predominant wear mechanisms and magnitude of the dimensional wear coefficient

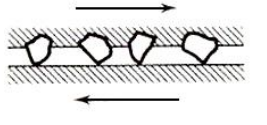
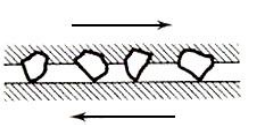
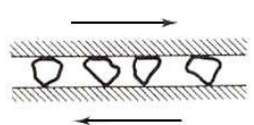
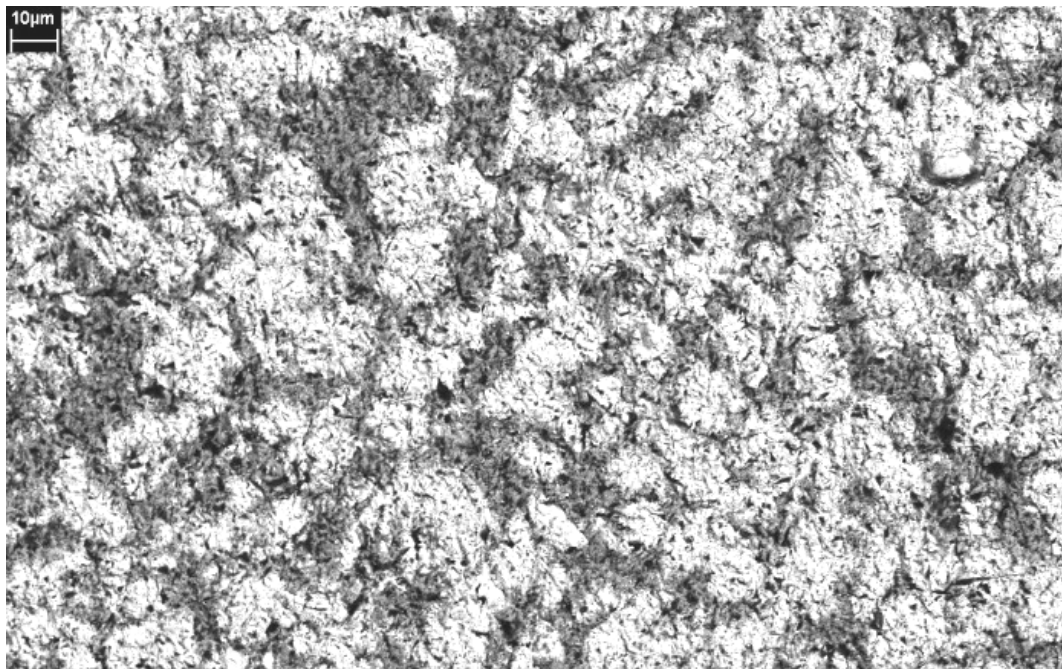
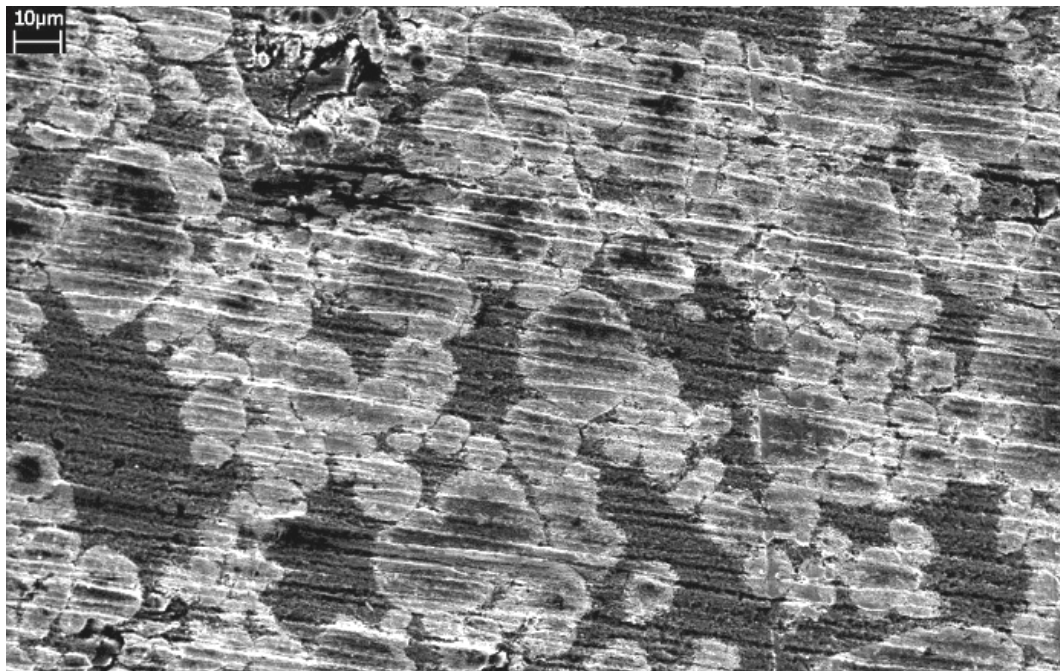
Slurry	Fe <sub>2</sub> O <sub>3</sub>	SiO <sub>2</sub>	SiC
Abrasive mean hardness	1000 HV	1100 HV	2600 HV
H <sub>A</sub> /H <sub>Brass</sub> ratio	3,9 ± 4 %	4,3 ± 4 %	10,2 ± 4 %
H <sub>A</sub> /H <sub>W</sub> ratio	1,3 ± 10 %	1,5 ± 10 %	3,4 ± 10 %
Wear Mechanisms	W = grooving Brass = Rolling (Multiple indentations) 	Grooving 	Rolling (Multiple indentations) 
K <sub>Fe<sub>2</sub>O<sub>3</sub></sub> /K....	1	0,12	0,02
K <sub>SiO<sub>2</sub></sub> /K...	8	1	0,13
K <sub>SiC</sub> /K....	66	8	1

Table 3 and Figures 4 and 5 indicate that, in general, SiC abrasive particles were responsible for rolling abrasion (multiple indentations) in all cases, and SiO<sub>2</sub> were associated with grooving abrasion in all cases.



**Figure 4** – Wear micromechanisms by multiple indentations. SiC slurry, SEM – backscattered electrons – matrix “4”.<sup>(3)</sup>



**Figure 5** – Wear micromechanisms by multiple indentations. SiO<sub>2</sub> slurry, SEM – secondary electrons – matrix “16”.<sup>(3)</sup>

More complex wear modes were observed in the case of the Fe<sub>2</sub>O<sub>3</sub> abrasive particles (Figure 6), which resulted in a mixed wear mode, predominantly with grooving abrasion on the tungsten particles and rolling abrasion on the infiltrated brass. In principle, this wear mode mixture may be explained when one notes that the hardness of Fe<sub>2</sub>O<sub>3</sub> is not significantly higher than that of the tungsten and is larger than that of the infiltrated brass.

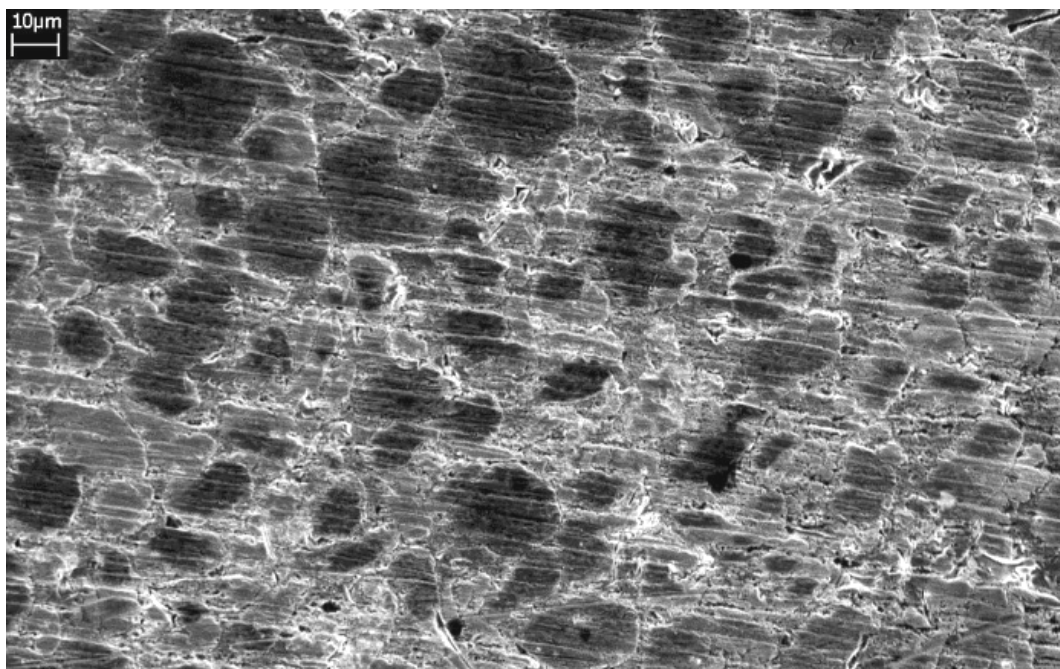


**Figure 6** – Wear micromechanisms by multiple indentations and grooving. Fe<sub>2</sub>O<sub>3</sub> slurry, SEM – secondary electrons – matrix “6”.<sup>(3)</sup>

For the tungsten particles, the greater the size the smaller the hardness value. The powder is produced by means of atomization technique, and the size of particle affects the cooling rate and consequently the hardness.

Tungsten particles hardness does not show a strong correlation with wear coefficient  $k$  for all abrasives. But, it can be said that the hardness has some influence in the wear rate for SiC and SiO<sub>2</sub> abrasives, figure 7 and 8. For the former abrasive, the higher the hardness the higher is the wear coefficient. In the case of the SiO<sub>2</sub>, the higher the hardness the lower is the wear coefficient. The tungsten hardness shows no effect on the wear coefficient for the Fe<sub>2</sub>O<sub>3</sub> abrasive (Figure 9).

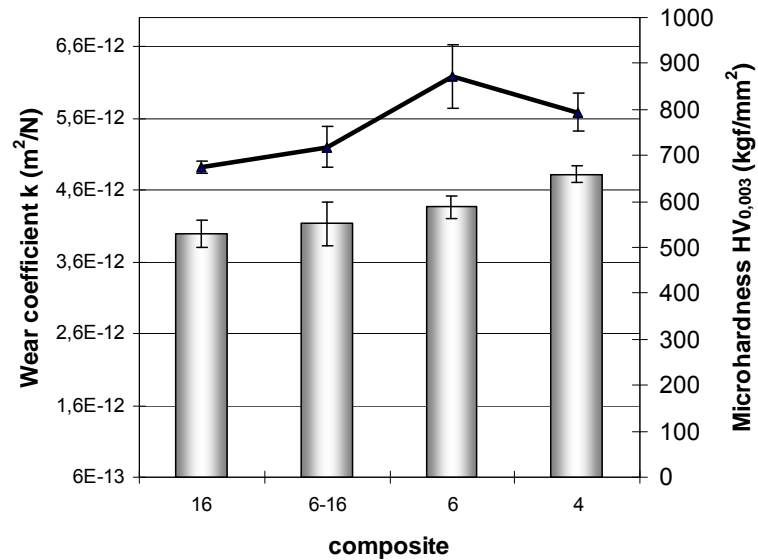


**Figure 7** – Relationship between the dimensional wear coefficient and the tungsten hardness for the SiC slurry.

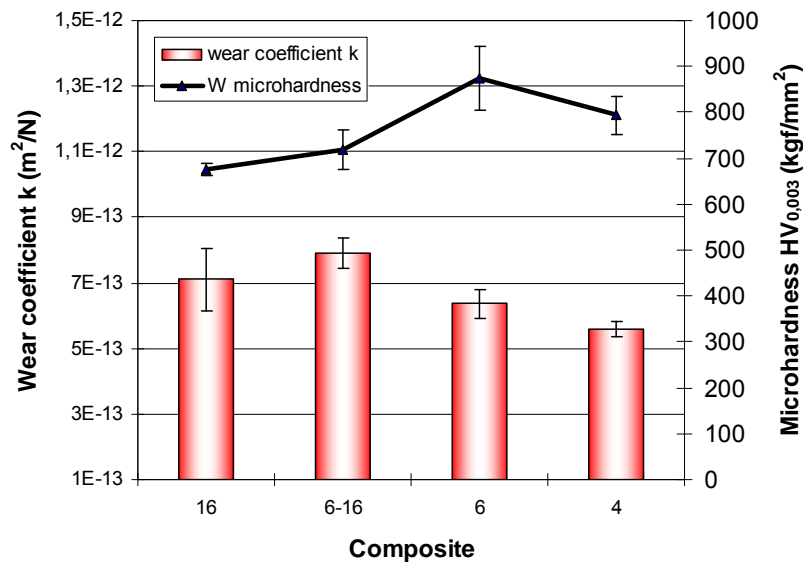


**Figure 8** – Relationship between the dimensional wear coefficient and the tungsten hardness for the SiO<sub>2</sub> slurry.



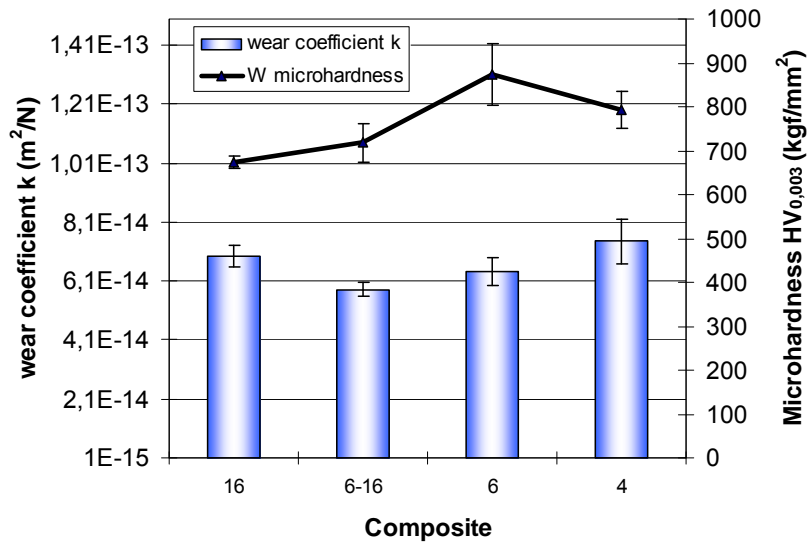


**Figure 9** – Relationship between the dimensional wear coefficient and the tungsten hardness for the Fe<sub>2</sub>O<sub>3</sub> slurry.

The infiltrated brass hardness shows a significant influence for the tests in SiO<sub>2</sub> and Fe<sub>2</sub>O<sub>3</sub> abrasive slurries, Figures 10 and 11, but has no effect on the SiC wear tests (Figure 12). In the latter, the H<sub>A</sub>/H<sub>B</sub> ratio is so high that the wear rate is not affected by the brass hardness. For SiO<sub>2</sub> e Fe<sub>2</sub>O<sub>3</sub> abrasives, the H<sub>A</sub>/H<sub>W</sub> ratio is closer to one so that the infiltrated brass hardness became an important parameter. For the SiO<sub>2</sub> abrasive the higher the microhardness of the brass the lower is the wear coefficient. For the Fe<sub>2</sub>O<sub>3</sub> slurry, the higher the brass microhardness the higher is the wear coefficient.

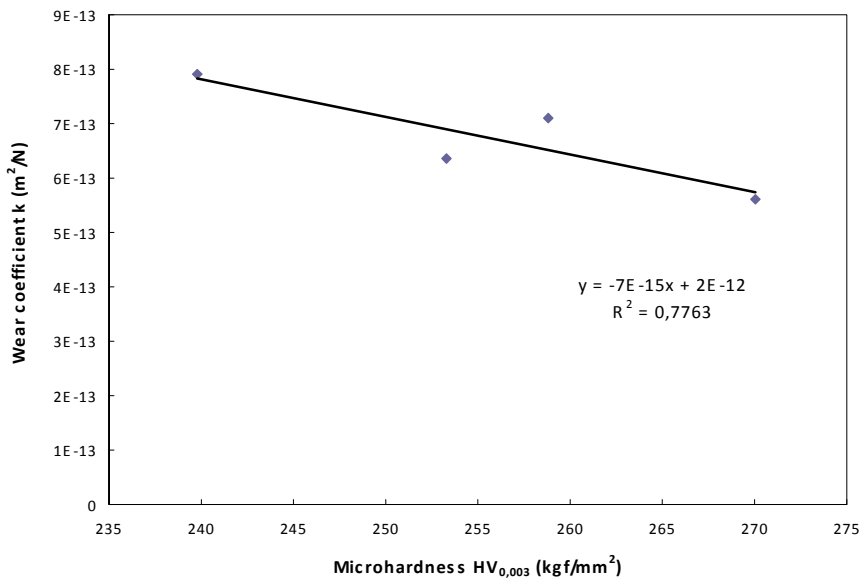


**Figure 10** – Relationship between the dimensional wear coefficient and the brass hardness for the SiO<sub>2</sub> slurry.

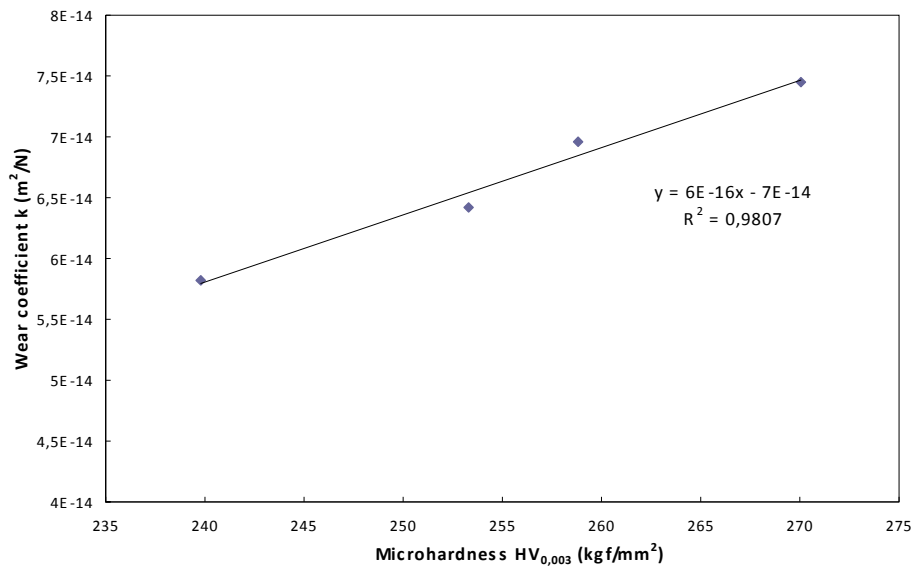


**Figure 11** – Relationship between the dimensional wear coefficient and the brass hardness for the Fe<sub>2</sub>O<sub>3</sub> slurry.

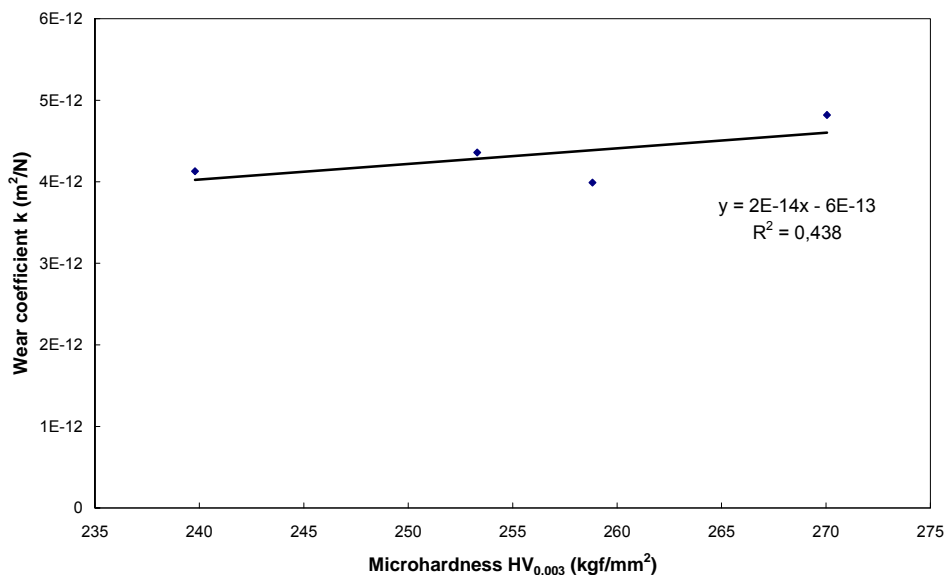


**Figure 12** – Relationship between the dimensional wear coefficient and the brass hardness for the SiC slurry.

## 4 CONCLUSIONS

1. Wear results present several orders of difference according to the type of abrasive particle. The wear severity is higher for SiC and the lower wear rate is obtained for Fe<sub>2</sub>O<sub>3</sub> particles.
2. It was observed different micromechanisms according to the type of abrasive. For SiC particles, rolling (multiple indentations) is the predominant micromechanism. Grooving is the most important mechanism for the SiO<sub>2</sub> slurry. A mixed mode (grooving abrasion on the tungsten particles and rolling abrasion on the infiltrated brass) was observed at the worn surfaces obtained from tests with Fe<sub>2</sub>O<sub>3</sub> slurry.
3. Tungsten particles microhardness varies with the particles size. A higher hardness was obtained for smaller tungsten particles.

4. The tungsten microhardness has some influence on the wear rate for SiC and SiO<sub>2</sub> abrasives. For the former abrasive, the higher the hardness the higher the wear coefficient. In the case of SiO<sub>2</sub>, the higher the hardness the lower the wear coefficient. The tungsten hardness shows no effect on the wear coefficient for the Fe<sub>2</sub>O<sub>3</sub> abrasive.
5. The infiltrated brass hardness shows a significant influence on the tests in SiO<sub>2</sub> and Fe<sub>2</sub>O<sub>3</sub> abrasive slurries, but has no effect on the SiC wear tests.

## REFERENCES

- 1 DWAN, J. D. Production of Diamond Impregnated Cutting Tools. **Powder Metallurgy**, v. 41, n. 2, p. 84-86, 1998.
- 2 DWAN, J. D. Manufacture of Diamond Impregnated Metal Matrixes. **Materials Science and Technology**, v. 14, p. 896-900, 1998.
- 3 LOZZER, A. M. **Microabrasão de compósitos de matriz metálica a base de tungstênio empregados em coroas de perfuração utilizadas em sondagem mineral**. Tese de Mestrado. Vitória, Espírito Santo, Brasil. UFES. 2008.
- 4 VANLANDINGHAM, M.R. Review of instrumented indentation. **Journal of Research of the National Institute of Standards and Technology**, v. 108, n. 4, p. 249-265, jul-aug. 2003.
- 5 HAY, J. C.; PHARR G.M. **Instrumented Indentation Testing**. In: Mechanical Testing and Evaluation. H. Kuhn and D. Medlin, Editors, ASM Handbook v. 8, ASM International, Materials Park, OH, 2000, pp. 232–243 (10th ed.)
- 6 SANTOS, S. G. **Avaliação do efeito de modificações superficiais a plasma no desempenho frente ao desgaste de um aço baixa liga: estudo da correlação entre profundidade de endurecimento e melhoria de desempenho**. Tese de Doutorado. Belo Horizonte, Minas Gerais, Brasil. Escola de Engenharia da UFMG. 2009.
- 7 OLIVER, W.C.; PHARR, G.M. An improved technique for determining hardness and elastic modulus using load and sensing indentation experiments. **Journal of Materials Research**, v. 7, p. 1564-1583. 1992.
- 8 MEZA, J.M.; MORE, M.C.; SOUZA, R. M.; CRUZ, L.J. Using the Ratio: Maximum Load over Unload Stiffness Squared,  $P_m/S_u^2$ , on the Evaluation of Machine Stiffness and Area Function of Blunt Indenters on Depth-sensing Indentation Equipment. **Materials Research**, v. 10, p. 437-447. 2007.